Passaro, M.; Cipollini, P.; Benveniste, J.. 2015 Annual sea level variability of the coastal ocean: The Baltic Sea-North Sea transition zone. *Journal of Geophysical Research: Oceans*, 120 (4). 3061-3078. 10.1002/2014JC010510

Passaro, M.; Cipollini, P.; Benveniste, J.. 2015 Annual sea level variability of the coastal ocean: The Baltic Sea-North Sea transition zone. *Journal of Geophysical Research: Oceans*, 120 (4). 3061-3078. 10.1002/2014JC010510

AGU PUBLICATIONS

JGR

Journal of Geophysical Research: Oceans

RESEARCH ARTICLE

10.1002/2014JC010510

Key Points:
- Coastal altimetry is able to analyze the annual sea level on a subbasin scale
- Wind is the main driver of the annual cycle in the whole area of study
- Steric effects and currents differentiate the annual cycle among the subbasins

Correspondence to:
M. Passaro,
marcello.passaro@noc.soton.ac.uk

Citation:
Passaro, M., P. Cipollini, and J. Benveniste (2015), Annual sea level variability of the coastal ocean: The Baltic Sea-North Sea transition zone, *J. Geophys. Res. Oceans*, *120*, 3061–3078, doi:10.1002/2014JC010510.

Received 16 OCT 2014
Accepted 14 MAR 2015
Accepted article online 23 MAR 2015
Published online 26 APR 2015

Annual sea level variability of the coastal ocean: The Baltic Sea-North Sea transition zone

M. Passaro[1,2], P. Cipollini[3], and J. Benveniste[2]

[1]Graduate School National Oceanography Centre Southampton, University of Southampton, Southampton, UK, [2]European Space Research Institute, European Space Agency, Frascati, Italy, [3]Marine Physics and Ocean Climate Research Group, National Oceanography Centre, Southampton, UK

Abstract The annual cycle is a major contribution to the nontidal variability in sea level. Its characteristics can vary substantially even at a regional scale, particularly in an area of high variability such as the coastal ocean. This study uses previously validated coastal altimetry solutions (from ALES data set) and the reference ESA Sea Level Climate Change Initiative data set to improve the understanding of the annual cycle during the Envisat years (2002–2010) in the North Sea-Baltic Sea transition area. This area of study is chosen because of the complex coastal morphology and the availability of in situ measurements. To our knowledge, this is the first time that the improvements brought by coastal satellite altimetry to the description of the annual variability of the sea level have been evaluated and discussed. The findings are interpreted with the help of a local climatology and wind stress from a reanalysis model. The coastal amplitude of the annual cycle estimated from ALES altimetry data is in better agreement with estimations derived from in situ data than the one from the reference data set. Wind stress is found to be the main driver of annual cycle variability throughout the domain, while different steric contributions are responsible for the differences within and among the subbasins. We conclude that the ALES coastal altimetry product is a reliable data set to study the annual cycle of the sea level at a regional scale, and the strategy described in this research can be applied to other areas of the coastal ocean where the coverage from the tide gauges is not sufficient.

1. Introduction

Sea level is a fundamental climate variable needed to understand the way the ocean interacts with climate fluctuations, and as such has been included in the Global Climate Observing System (GCOS) list of Essential Climate Variables (ECVs). One of sea level's most prominent periodic variations is the annual component, which is affected both by steric effects (changes in water density) and mass variations. The amplitude and phase of the annual cycle are related to the seasonality of a wide range of phenomena: warming/cooling of sea water, precipitation, rivers runoff, seasonal atmospheric processes, and ocean circulation [*Barbosa et al.*, 2008]. Measured annual cycle amplitudes range from a few centimeters to almost 30 cm depending on the region of the world [*Vinogradov et al.*, 2008]; the phase therefore has an important effect during extreme sea level events, when storm surges combine with tides and mean sea level.

The steric contribution to the annual sea level signal is known to be prevalent in the deep ocean, while in coastal regions complex bathymetry, local circulation, and forcing from rivers, atmosphere, and wind can be more significant. The variables that affect the annual cycle are often characterized by strong spatial gradients in coastal regions and previous studies have demonstrated that the annual cycle characteristics can change from open ocean to coast [*Vinogradov and Ponte*, 2010]. Coastal sea level variability is therefore the most challenging to interpret, and also to measure. The most reliable and frequent measurements come from tide gauges (TGs), but their coverage is not global and they do not provide a description of the changes that intervene between coast and open ocean.

For more than two decades, satellite radar altimetry has been providing global along-track measurements of sea level, with an accuracy of 2–3 cm for averaged estimations every 7 km along a track [*Bonnefond et al.*, 2011]. Benefiting from multiple altimetry missions, oceanographers have been able to describe global sea level variability and long-term trends. However, the confidence in altimetry data decreases toward the

coast. Until recently, data closer than 50 km from land have been considered unreliable, mainly due to two factors:

1. The corruption of ocean returned echoes by land and calm patches of coastal waters with high reflectivity.
2. The unreliability of the corrections needed to isolate the sea level anomaly signal from the altimetry measurement.

In recent years, efforts have been made to provide solutions to address both problems [*Vignudelli et al*., 2011]. The first issue is related to "retracking," i.e., the on-ground process that leads to more precise estimations of the parameters that can be extracted from an altimetric echo: sea level, significant wave height (SWH), and wind speed. In this study, the retracking strategy of choice is ALES, the Adaptive Leading Edge Subwaveform Retracker [*Passaro et al*., 2014, 2015]. ALES has been applied to past and current altimetry missions (Envisat, Jason 1, Jason 2, AltiKa) and has been validated in areas of the world with different characteristics, showing a consistent improvement compared to standard products in the coastal areas and similar performances in the open sea.

The second issue is related to contributions from different corrections. The solutions adopted in the study will be described in section 3. The most problematic corrections for coastal data are known to be:

1. The wet troposphere correction, which accounts for the delay of the radar signal by water vapor in the atmosphere.
2. The tidal model, i.e., the correction used to extract the part of sea level variability due to astronomical tides.
3. The dynamic atmospheric correction, i.e., the ocean response to high and low-frequency variations in meteorological forcing (atmospheric pressure and wind).

The aim of our study is to verify whether the ALES-based coastal satellite altimetry product is able to improve the description of the annual cycle of the sea level in the coastal ocean on subbasin scales (10–100 km) and, in combination with information from different sources, to identify the processes that drive the variability.

To answer this question, the study focuses on the transition zone between the North Sea and the Baltic Sea. The area is characterized by challenging conditions for satellite altimetry. The jagged coastline and several islands are potential sources of corruption for altimetry measurements, while shallow water areas are known to be particularly critical for tidal patterns (due to shallow water components and nonlinear tides). Nevertheless, the high number of reliable TGs makes the area an ideal test for coastal sea level variability studies. Up to now, sea level description of the area has mainly focused on in situ data [*Wahl et al*., 2013; *Stigebrandt*, 1984]. The first attempt to use coastal altimetry in the area was performed by *Madsen et al*. [2007], although avoiding data closer than 10 km from the coast, while other studies limited the use of altimetry to the open sea [*Novotny et al*., 2006]. More recently, *Stramska* [2013], *Stramska and Chudziak* [2013], and *Stramska et al*. [2013] used Sea Level Anomalies (SLA) extracted from a multimission global gridded data product in the open Baltic and North sea, underlining that further developments in coastal altimetry could lead to improvements in the description of the sea level variability. Our study follows this path, including and evaluating the contribution of along-track measurements in the coastal zone.

This research is based on ALES reprocessed Envisat data in comparison with the up-to-date sea level product generated by the ESA Sea Level Climate Change Initiative (SL_cci) community, which is an international effort to provide the most reliable and freely available information on the Sea Level ECV, but which has not specifically generated coastal products yet. To our knowledge, our study is the first to investigate the sea level seasonality using along-track satellite altimetry up to the coast with a dedicated retracked altimetry data set. Further description on the area of study is given in section 2. Section 3 presents the data sets that have been used in the study. Section 4 describes the methodology used to process the measurements and estimate the sea level variability. In section 5, the results are presented and discussed. Section 6 draws the conclusions and the outlook for future research.

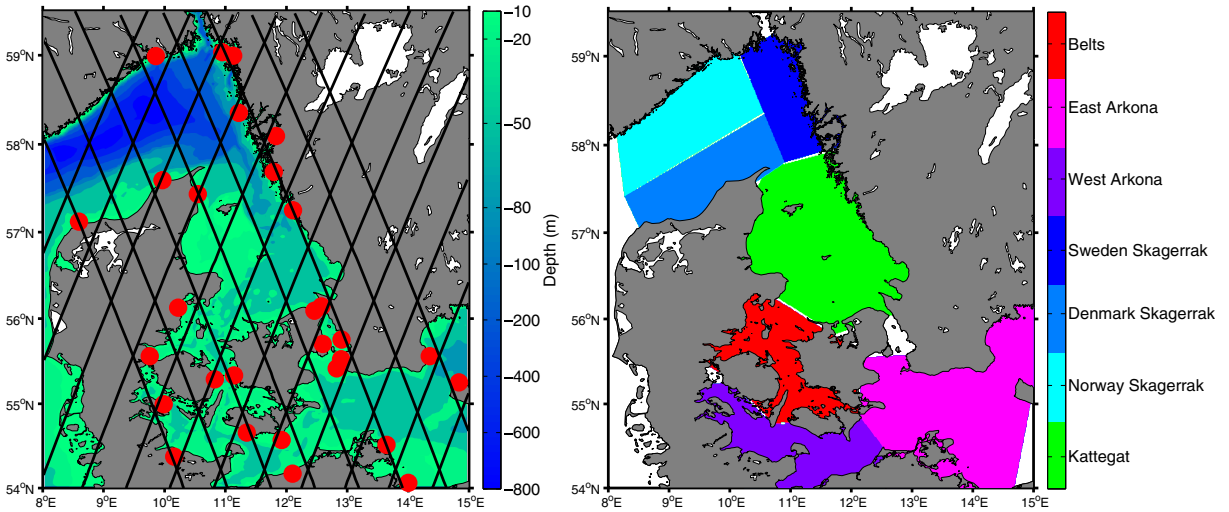

Figure 1. The area of study. (left) The red circles are the locations of the TGs and the black lines are the Envisat tracks. (right) The subbasin is defined and color coded. Color scale is linear between 0 and −100 and then linear but with different slope between −100 and −800.

2. Area of Study

Our area of study is shown in Figure 1. We have divided the area into subbasins, based on different oceanographic characteristics. To the west, it includes the Skagerrak Sea, characterized by a mainly cyclonic circulation influenced by the topography (see *Svendsen et al.* [1996] for a map showing the mean features of the circulation). The southernmost part of the subbasin (D Skagerrak) is shallow, like most of the North Sea, but the northern area (N Skagerrak) is characterized by the deep Norwegian Trench [*Winther and Johannessen*, 2006]. A wide surface current coming from the west carrying waters from the Atlantic and the German Bight (Jutland Current) turns northward when it encounters the brackish water from the Baltic Sea and follows the Norwegian coast, being named Norwegian Coastal Current (NCC). To the south, the Kattegat Sea is a shallow sea characterized by estuarine processes, namely the mixing of salty Atlantic water with brackish water from the Baltic Sea and freshwater from rivers [*Winther and Johannessen*, 2006]. The inflow and outflow of water through the Danish straits (the Belts subbasin) depends on the sea level difference between the Kattegat Sea and the Arkona basin (the westernmost part of the Baltic Sea) [*Samuelsson and Stigebrandt*, 1996]. The mean flow condition across the straits, i.e., an upper brackish water layer flowing from the Baltic Sea to the Kattegat Sea and an opposite flow in deeper waters, can be altered by local wind conditions and larger atmospheric circulation patterns [*Lehmann et al.*, 2002]. In this study, the easternmost strait (Oresund) is left out due to the lack of altimetry tracks in the area. Finally, the Arkona Basin is mainly characterized by a decreasing salinity from west to east [*Liebsch et al.*, 2002]. More detailed descriptions of the circulation in this area can be found in *Holt and Proctor* [2008], *Maslowski and Walczowski* [2002], and *Lass and Mohrholz* [2003].

3. Data Set

The main source of data we use in this study is satellite altimetry. Here we focus on data from the ESA Envisat mission, which we have reprocessed with ALES. The data we use cover Envisat orbital Phase B, from autumn 2002 to the 22 October 2010, the date on which the Envisat orbit was changed. Tracks are repeated every 35 days. This limits the amount of data along repeat tracks, but makes the Envisat mission particularly suitable for regional studies of seasonal phenomena, due to the high spatial coverage of the tracks (see Figure 1) compared to the Jason series, which have a 10 day repeat time, but a larger distance between the tracks. Envisat Sensor Geophysical Data Records (SGDR) have been downloaded through the Earth Online (EO) User Services. They provide high-rate averaged waveforms at 18 Hz, including all the available

corrections applied to the standard product. A description of the coastal degradation of these standard corrections can be found in *Andersen and Scharroo* [2011].

The wet tropospheric correction obtained by microwave radiometer measurements is not reliable in the coastal zone: the radiometer 3-dB footprint has a diameter of 21.2–22.5, depending on the antenna frequency, but the effect of land intrusion in the footprint is already significant at 30–50 km from the coast in terms of the error it induces on the correction [*Envisat-1 Products Specifications*, 2009; *Joana Fernandes et al*., 2013]. In the SGDR, a modeled correction is available, based on the European Centre for Medium-Range Weather Forecasts (ECMWF) model, but its resolution is suboptimal: the temporal resolution is 6 h, but the tropospheric water content can vary at shorter temporal scales, while the maximum spatial resolution (from the operational model) is $0.12\times0.12^{\circ}$, i.e., smaller than the satellite resolution [*Legeais et al*., 2014]. For this study, the GNSS-based Path Delay (GPD) wet tropospheric correction has been used. The GPD correction has been produced by the group led by J. Fernandes at the University of Porto, as part of the ESA SL_cci project [*Joana Fernandes et al*., 2010]. The GPD correction combines the tropospheric path delays from Global Navigation Satellite System (GNSS) measurements at inland coastal stations with the valid values of Wet Tropospheric Correction computed from the Microwave Radiometer on board Envisat and with the output of a numerical weather model. It is fully compatible with the microwave radiometer-based correction (used in the open ocean) and guarantees consistency in the transition from open ocean to the coastal zone. More detailed description and validation of the results is found in *Joana Fernandes et al*. [2010].

The tide correction and the mean sea surface (MSS) already available in the SGDR have been substituted with validated up-to-date products: the DTU10 global tide model, particularly suitable for shallow seas, and the DTU13 mean sea surface [*Andersen*, 2010; *Cheng and Andersen*, 2011]. MSS choice was driven by the need to harmonize the set of corrections applied in the products: since the DTU model was already the choice of the validated ALES product as well as of the CCI product, this choice was kept. DTU10 tide model was preferred to GOT 4.8 (model of choice in the gridded SL_cci) and applied to ALES and CCI along-track data due to the less favorable statistics of GOT against shallow tide gauges and erroneous values of the correction in the Danish seas, as well as the good performances of the DTU model, as recently shown by *Andersen et al*. [2014] and *Stammer et al*. [2013].

In order to isolate the response of the ocean to atmospheric forcing in terms of sea level, both the low-frequency response to variations in atmospheric pressure (with periods of half a day or longer, known as the "inverse barometer correction") and the high-frequency atmospheric forced variability (such as wind effects) have to be taken into account. This "atmospheric correction" has to be applied to both TGs and altimetry data, and therefore, a common source is needed. This is provided by the Dynamic Atmosphere Correction (DAC) [*Carrère and Lyard*, 2003]. In the version applied to ALES data, the MOG2D barotropic atmospheric model is forced by the ECMWF (European Centre for Medium-Range Weather Forecasts) operational analysis (with inputs every 6 h) and has a spatial sampling of $0.25^{\circ} \times 0.25^{\circ}$.

In order to compare our results with the latest altimetry products, the same analysis described in section 4.2 has been applied to gridded altimetric data (Level 4) and to Envisat along-track data (Level 2) from the ESA SL_cci project. The gridded product consists of a 1/4-of-degree regular spaced grid with monthly sea level anomalies that combine all the available satellite altimetry data (Jason-1/2, Envisat, ERS-2, Topex/Poseidon and GFO missions in our time span), while the along-track product is directly comparable with ALES data, since the two products refer to the same points in time and space.

In the DAC correction applied to the SL_cci data set, MOG2D is forced by ERA-Interim atmospheric reanalyses, which guarantees stable performance over the time, but at a lower spatial resolution ($0.75^{\circ} \times 0.75^{\circ}$). Since the two corrections have generally equivalent performances from 2002 onward and since higher spatial resolution is appropriate in the coastal ocean, the operational ECMWF-based DAC is applied in this study to both ALES and Envisat SL_cci data sets. The gridded SL_cci product provides sea level anomalies and therefore, given that a gridded version of the ERA-interim-based DAC is not yet available, it was not possible to change its atmospheric correction. As previously mentioned, the gridded SL_cci applies a tide correction generated from the GOT 4.8 tidal model, while mean sea surface (DTU13) and wet tropospheric correction (GPD) are the same as in ALES.

To add further consistency to the improvements seen by ALES, which will be described in the next sections, we also performed the same analysis on the 1 Hz Envisat sea level estimations from the Radar Altimetry

Database System (RADS, http://rads.tudelft.nl/) [*Scharroo et al*., 2012]. By doing so, it is possible to verify that the improvements are not, or not only, due to the fact that ALES does not apply postprocessing techniques (such as filtering and merging) adopted in the CCI framework, which are suitable for open ocean, but may be not in the coastal environment. The same corrections of ALES were applied to RADS estimations as well, without any further screening of the data. Although most of the plots and discussions of the next sections do not involve this data set, the corresponding statistics are shown in Tables 2–4.

In situ observations of sea level are provided by the TGs. Here we use monthly mean sea level time series at all available TG sites in the study area from the Permanent Service for Mean Sea Level (PSMSL).

To derive the annual cycle of the steric component (section 4.2), we have computed the mean monthly temperature and salinity profiles using the in situ observations from the KLIWAS gridded climatological data set [*Bersch et al*., 2013].

Wind stress is obtained from the monthly gridded data of NCAR/UCAR Simple Ocean Data Assimilation (SODA) reanalysis. The information on wind stress comes from Twentieth Century Reanalysis (CR20 v2) and is provided in a $0.5^\circ \times 0.5^\circ$ grid [*Giese and Ray*, 2011].

4. Methods

4.1. Data Reprocessing

SGDR high-rate waveforms from Envisat missions have been reprocessed with the ALES retracker. Corrections for dry/wet troposphere, ionosphere, sea state bias, dynamic atmosphere effects, and tides were applied to the resulting 18 Hz range estimations in order to extract the sea level height anomaly (SSHA).

The high-rate measurements were interpolated onto nominal tracks, as described in *Passaro et al*. [2014]. From high-rate waveforms, ALES retracked sea level was then averaged to generate 1 Hz estimations. Four checks were performed in order to eliminate outliers in the following order:

1. The coastal proximity parameter (CPP) corresponding to the Envisat nominal track points was extracted from the global CPP data file computed at the National Oceanography Centre Southampton (NOCS) in the context of the ESA SL_cci project. This parameter quantifies the influence of land (taking in consideration not only the distance from the coast, but also its morphology) on the radar returned echoes, and varies from -1 (typical open ocean scenario with no land effects) to $+1$ (full inland, no return from sea). In this study, points with a CPP value from 0 to 1 were excluded. A CCP of 0 can be considered as a "virtual coastline" that delimits the point where, for retracking considerations, the returns from sea and land have equal effect (see *Cipollini* [2011] for a detailed description).
2. Every ALES retracked 18 Hz waveform is characterized by a fitting error on the leading edge. The fitting error is a measure of how close the fitted waveform is to the real signal and corresponds to the normalized square root of the difference between the modeled waveform and the real signal along the leading edge. Estimations that had a fitting error of over 0.5 (normalized power units) were excluded.
3. Considering that the tidal signal has been removed from the SSHA, 18 Hz estimations outside $[-3m, +3m]$ in absolute value were considered outliers and excluded.
4. The median value and the scaled median absolute deviation ($\widehat{MAD}$) were computed. Each estimation, x, was considered valid if:

$$x < median(X) + 3 \times \widehat{MAD}(X)$$

or

$$x > median(X) - 3 \times \widehat{MAD}(X)$$

where

$$\widehat{MAD}(X) = 1.4286 \times median(|X - median(X)|)$$

and X is the vector containing the 20 high rate estimations that are used to form a 1 Hz point. The $\widehat{MAD}$ scaled using the factor 1.4286 is approximately equal to the standard deviation for a normal distribution.

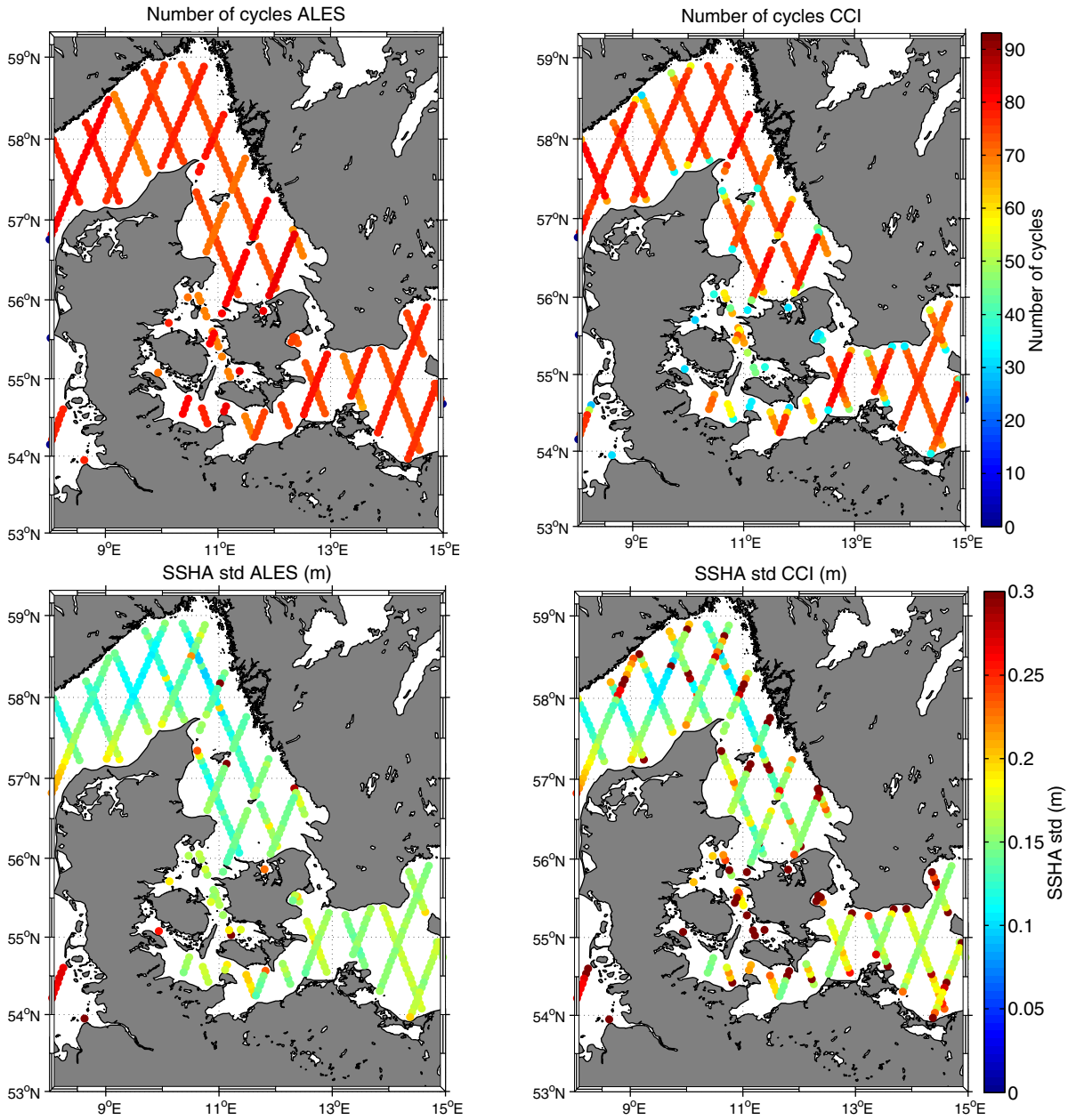

Figure 2. Comparison between (left) ALES reprocessed and (right) Envisat SL_cci data sets in terms of (top) number of cycles available and (bottom) standard deviation of the SSHA time series for each 1 Hz location.

Statistics based on the median are more robust and suitable for outliers detection and have been previously applied to satellite data [*Alvera-Azcárate et al.*, 2012]. Once the outliers had been excluded, the median of the remaining points was computed in order to generate the 1 Hz estimation.

Throughout the study, SSHA altimetry time series are formed at various distances from the coast and grouped depending on the geographical definition of each subbasin. Since the Envisat ground track velocity is about 7 km/s, the sea level measurements from the same cycle and pass are considered to be simultaneous. Therefore, each estimate in the time series corresponds to the median SSHA of all the 1 Hz points from the same pass that fall in the considered geographical interval.

TG data were also grouped depending on the corresponding subbasin. Since the sea level measured at each TG is relative to a local benchmark, the mean value of all the estimations was subtracted from each

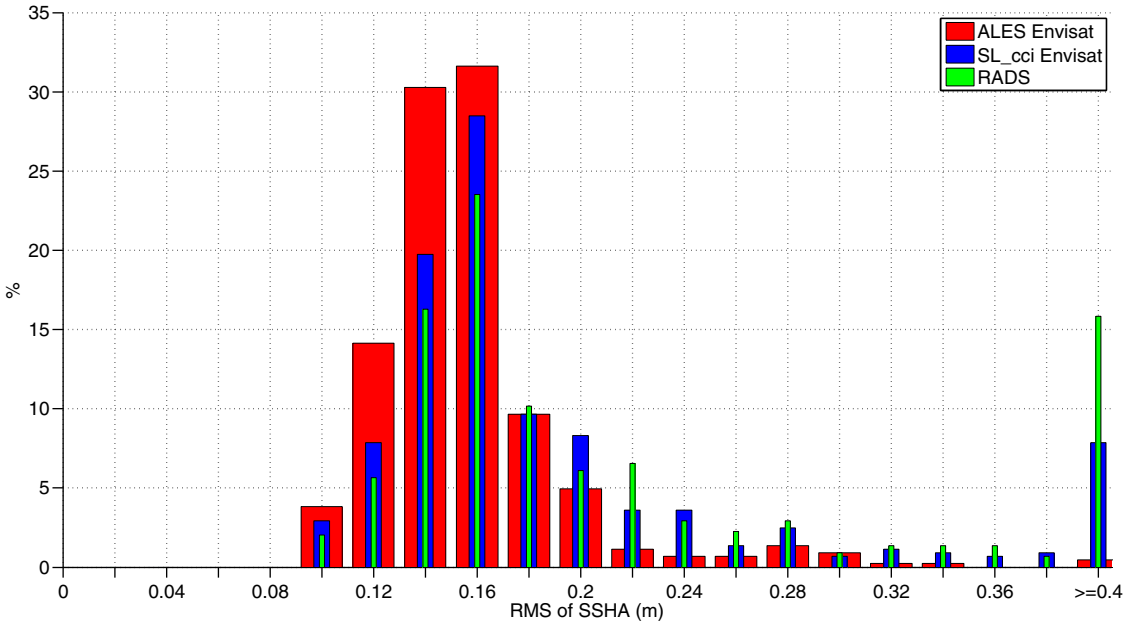

Figure 3. Histogram of the root mean square of SSHA computed at each 1 Hz location from ALES reprocessed (red), Envisat SL_cci (blue), and RADS (green) data sets.

monthly average. Time series of sea level from altimetry and PSMSL data are compared in Figure 4. For this comparison, in order to remove the short-term fluctuations, altimetry data were grouped into monthly means and a 3 month running mean filter was applied to both the data sets.

4.2. Estimation of the Annual Cycle

To estimate the annual cycle for all the considered data sets, a harmonic analysis of the time series was performed. The parameters are estimated by a least squares minimization analysis that compares the model with the time series. In particular, this study adopts the Prais-Winsten (PW) estimator [*Prais and Winsten*, 1954], which accounts for the problem of autocorrelation of the residuals in geophysical time series.

4.3. Estimation of the Steric Height

In order to obtain the steric component of the annual cycle of the sea level, the steric height needs to be derived from the temperature and salinity data at each depth using a climatology. The steric height is related to the ocean density: applying the equation of state described by *Gill* [1982], a density profile at each sampled location was derived from the records of temperature and salinity. The assessment of the steric sea level variations from the density profiles is based on the integral method described in detail by *Tomczak and Godfrey* [2003], *Jayne et al*. [2003], and *Lombard et al*. [2005]. To discriminate the thermosteric and the halosteric components, we have followed the methodology described in *Ivchenko et al*. [2007].

5. Results and Discussion

5.1. Altimetry Data Quality

A preliminary analysis is conducted on the two along-track altimetry data sets. Figure 2 shows the improvements of reprocessed altimetry compared to the SL_cci data set in terms of quantity and quality of the data. The top plots show the number of the available cycles in both the data sets. It is important to stress that at this stage, ALES data have already been quality controlled and therefore the statistics represent the number of measurements that are then used in the sea level analysis. Envisat SL_cci has gaps in the Belts and Arkona basins, as well as within 15 km of the coast in the whole domain. ALES includes all the available cycles and the only missing points are due to passes where no waveforms are available in the SGDR files. The availability is uniform across the whole domain.

An increased amount of data is not helpful if the quality of the retrievals is poor. As a first evaluation, the bottom plots of Figure 2 show the standard deviation (std) of the SSHA time series at each 1 Hz location. In

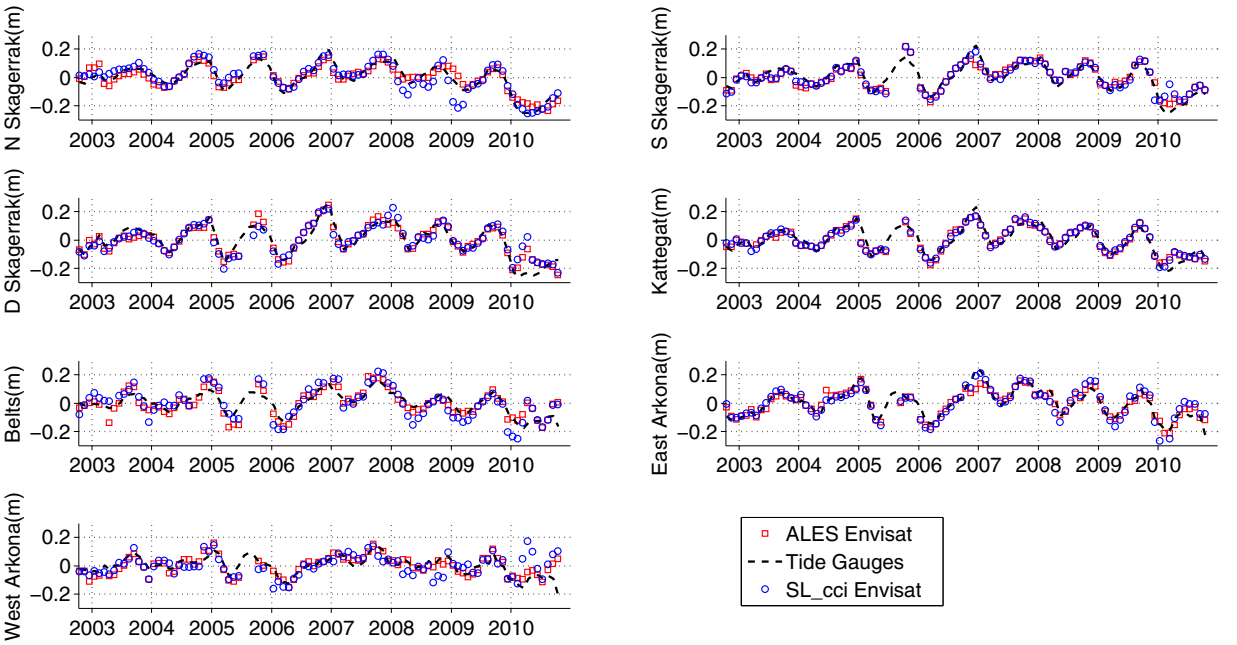

Figure 4. Monthly averages of SSHA (with 3 month running mean filter applied) grouped by subbasin, from TGs (black dashed line) and satellite altimetry within 15 km of the coast for ALES reprocessed data set (red squares) and Envisat SL_cci (blue circles).

order to be consistent, the std of SSHA is expected to vary smoothly with no abrupt changes between consecutive 1 Hz points. This is verified in ALES with the exception of very few unrealistic values. The Envisat SL_cci data set shows evident signs of corrupted estimations. The most problematic areas are again the Arkona basin, the Belts, and the last 15 km from the coast, but unrealistic variability in the SL_cci SSHA values is seen also in the Skagerrak and Kattegat open seas.

The histogram in Figure 3 shows the distribution of the root mean square (rms) of the SSHA time series at each 1 Hz point in the area of study. The variability of ALES is slightly smaller than the Envisat SL_cci. Overall, SL_cci has more locations where the rms level is higher than the average variability in the area and in particular more than 7% of the points with an unrealistic rms larger than 40 cm. The histogram shows also the rms from RADS data set, which performs worse than the others, proving that dedicated retracking and postprocessing are able to increase the overall quality of the estimations.

5.2. Time Series of Sea Surface Height Anomaly

Averaged time series of SSHA from TGs and 1 Hz altimetry locations within 15 km of the coast are shown for each subbasin in Figure 4. There is good agreement between the in situ and the remotely sensed sea level. Correlation coefficients between the time series are listed in Table 1. ALES data are better correlated with TGs than Envisat SL_cci data across the whole area of study, except a 0.01 improvement in the correlation of Envisat SL_cci in the Kattegat Sea.

Table 1. Correlation (CORR) Coefficient Between Altimetry and Tide Gauges (TG) Sea Level Monthly Averaged Time Series for Each Subbasin[a]

Subbasin	CORR ALES—TG	CORR SL_cci—TG
Kattegat	0.92	0.93
Norway Skagerrak	0.91	0.89
Denmark Skagerrak	0.92	0.86
Sweden Skagerrak	0.91	0.9
West Arkona	0.82	0.48
East Arkona	0.92	0.91
Belts	0.85	0.82

[a]Three-months running mean filter is applied.

Table 2. Mean Crossover Differences of the Annual Cycle of the Sea Level (Amplitude) for Each Subbasin

Subbasin	ALES (m)	SL_cci Env (m)	RADS (m)
Kattegat	0.024	0.056	0.053
Norway Skagerrak	0.037	0.035	0.037
Denmark Skagerrak	0.041	0.040	0.035
Sweden Skagerrak	0.001	0.031	0.031
West Arkona	0.040	0.022	0.057
East Arkona	0.012	0.016	2.767
Belts	0.008	0.022	0.003

The Skagerrak, the Kattegat, and the East Arkona subbasins show a very similar behavior and the annual signal dominates their variability, while this periodicity is less evident in the Belts and the West Arkona subbasins. Even in these two regions though, the TGs and ALES coastal altimetry time series show good agreement, with correlation coefficients above 0.8, while Envisat SL_cci data are poorly correlated with the in situ time series of West Arkona. In all the area of study, even over the short time scale assessed, there are significant inter annual variations. In particular, from the middle of 2006 to the end of 2008, the anomalies are almost constantly of positive sign.

Past studies [*Stigebrandt*, 1984; *Ekman*, 2009; *Stramska*, 2013] have shown the importance of the wind patterns and their fundamental role in the transfer of water masses. Winds in the area are westerlies, easterlies, or southeasterlies but the westerly winds are predominant and reach their highest speed in Autumn and Winter, when the passing of low-pressure systems increase the storm activity [*Karagali et al.*, 2014]. Westerlies bring water from the North Sea and the Atlantic into the Skagerrak and the Kattegat Sea, while easterlies drive the outflow into the North Sea. In this study, coastal altimetry data within 15 km from the coast confirm the variability of the sea level in the annual time scale due to persistent winds redistributing waters: Figure 5 provides a verification by comparing the monthly averaged ALES reprocessed SSHA of the Swedish Skagerrak coast with the monthly averaged zonal wind stress in the entire Skagerrak area. The two curves have a correlation coefficient of 0.63, which is a significant indication of the influence of wind patterns on sea level. All the maxima in the sea level coincide with strong westerly wind events and the lowest SSHA are found during easterlies. The time of appearance of strong westerlies act as a phase regulator for the sea level. For example, in 2004/2005 and 2006/2007 winters, the time of high sea level and strong westerlies is December/January, while in 2008/2009 and 2009/2010 this happens in October/November. January of 2010 is the month with the strongest negative anomalies of sea level and coincides with the strongest easterlies found in the time series.

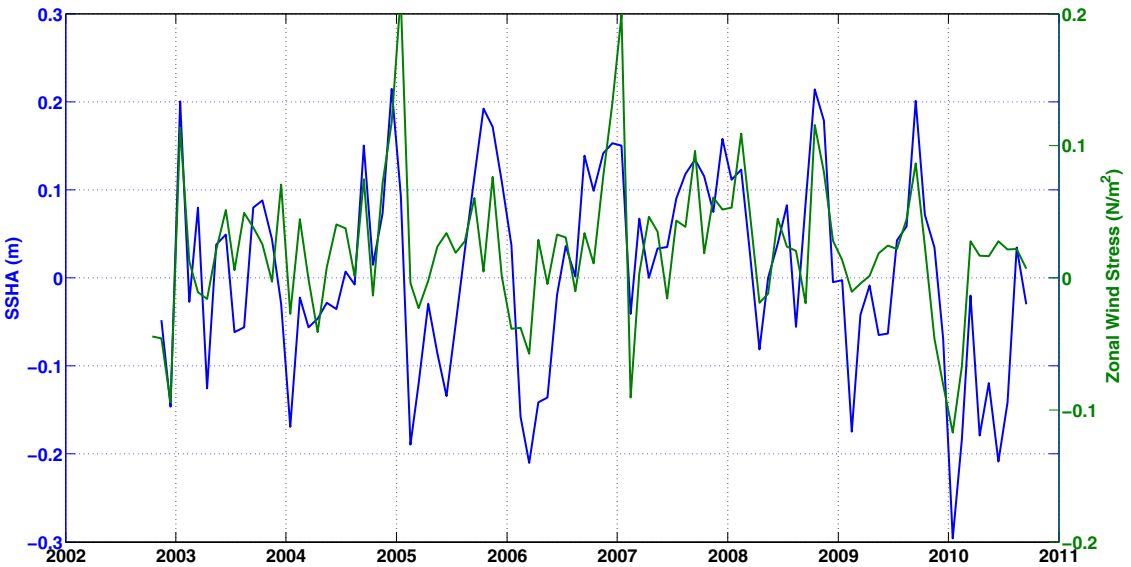

Figure 5. Monthly averages of zonal wind stress from Twentieth Century (CR20 v2) Reanalysis (in green) and of SSHA (in blue) from ALES data set within 15 km of the coast in Swedish Skagerrak.

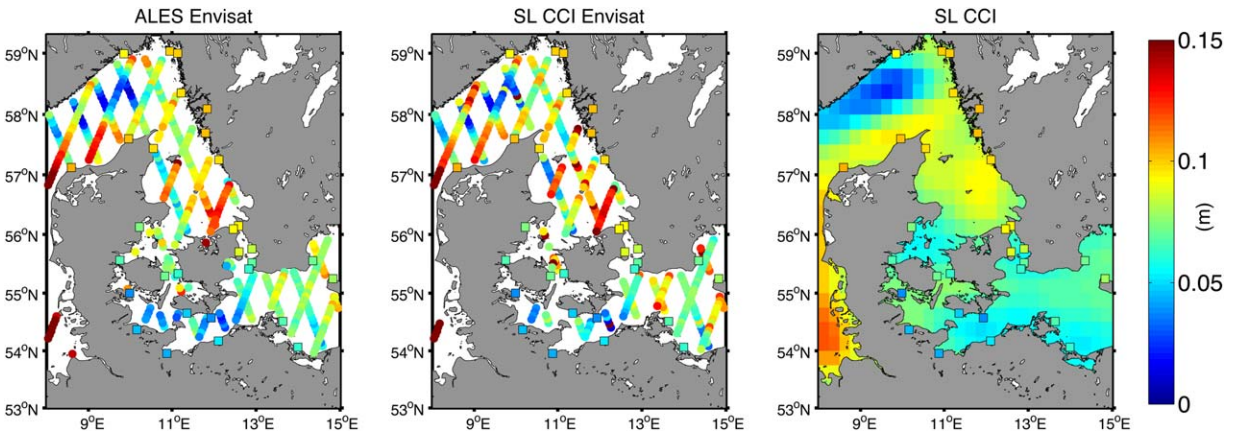

Figure 6. Estimates of annual cycle amplitude from TG data (squares) and 1 Hz altimetry points along the Envisat tracks for (left) ALES reprocessed data set and (middle) Envisat SL_cci. (right) The estimates from gridded SL_cci.

5.3. Pointwise Estimation of the Annual Cycle

In this section, we assess the spatial variability of the annual cycle and the ability of Envisat to capture it. Figure 6 shows the amplitude of the annual cycle derived at each 1 Hz point of the tracks for ALES reprocessed data set and Envisat SL_cci and at each grid point of the merged SL_cci data set. The corresponding estimates from the TG data are shown on the figure with squares. For the along-track altimetry, only 1 Hz points where at least 5 years of data are available (∼50 Envisat cycles) have been included, which is why the Envisat SL_cci does not have some coastal estimations and there are voids in Belts and West Arkona.

Since for the pointwise analysis, we are generating time series with a frequency of one measurement every 35 days, the estimated annual cycle will include the contribution coming from any error in the tidal correction for the K1 constituent (which has an aliasing period of 365.24 days) [*Volkov et al.*, 2012]. Nevertheless, the estimations used for validation, coming from TGs that measure the sea level every few minutes, are not affected by this aliasing.

The annual signal in the Belts and Arkona regions shows a marked difference from the Kattegat/Skagerrak in terms of amplitude, which is well captured both in ALES and in the merged SL_cci, although the merged SL_cci data overestimate the amplitude in the westernmost part of the West Arkona area. As the merged product used a different tidal model, this discrepancy may be caused by unresolved tidal signal.

Table 2 shows, for each subbasin, the average difference in the amplitude estimation of the annual cycle at the crossovers. ALES improves the statistics by a factor of 2 or more in the Kattegat and in the Belts; it is the only data set to have a crossover agreement below the centimeter level (in the Swedish Skagerrak and in the Belts). The Envisat SL_cci improves the agreement by a factor of 2 in the only crossover point of the West Arkona. The table also shows the statistics for RADS, whose performances are generally worse than ALES and similar to SL_cci, although results are significantly worse in the Arkona Basin and marginally better (∼0.5 cm) in the Danish Skagerrak and in the Belts.

Areas of disagreement between ascending and descending tracks are present in both ALES and Envisat SL_cci CCI data sets, particularly along the Danish coasts, where the ascending tracks estimate higher amplitude compared to the descending ones. These differences are caused by the intrinsic problem of using a single point along an Envisat track to estimate the annual cycle: since Envisat has a sun-synchronous orbit, ascending passes and descending passes respectively cross the equator at 10 P.M. local time and 10 A.M. local time. Errors in the corrections that have a daily cycle can affect the crossover differences and this is particularly true for errors in the K1 tidal constituent, since they are aliased in the annual cycle [*Faugere et al.*, 2006].

Table 3 reports the mean difference in the amplitude estimation of the annual cycle estimated by the tide gauges and the closest 1 Hz altimetry point for each subbasin. The estimates at each 1 Hz point are less accurate than the subbasin averages, due to the relatively small number of repeated observations: the multimission merged SL_cci scores slightly better, benefiting from the optimal interpolation of more

Table 3. Mean Difference of the Annual Cycle of the Sea Level (Amplitude) Estimated by the Tide Gauges and the Closest 1 Hz Altimetry Point for Each Subbasin

Subbasin	ALES (m)	SL_cci Env (m)	SL_cci (m)	RADS (m)
Kattegat	0.026	0.067	0.016	0.153
Norway Skagerrak	0.027	0.013	0.021	0.012
Denmark Skagerrak	0.029	0.029	0.014	0.029
Sweden Skagerrak	0.023	0.023	0.020	0.016
West Arkona	0.022	0.020	0.022	0.211
East Arkona	0.012	0.028	0.008	1.630
Belts	0.013	0.015	0.007	0.093

measurements from missions with different sampling characteristics. ALES scores better than or equal to Envisat SL_cci in all basins except the Norwegian Skagerrak, although the comparison is affected by the fact that the Envisat SL_cci does not include some of the coastal 1 Hz locations due to the lack of data. The last column of the table reports the statistics for RADS. Performances are significantly worse in four subbasins, with differences of over 10 cm compared to the tide gauges, while RADS scores better than ALES within a cm level in the Skagerrak Sea.

In the along-track data sets, a slope in the amplitude of the annual cycle is visible in the Skagerrak Sea, with higher values near the coast and low values in the open sea. The change matches the change in bathymetry. The area of low amplitude of the annual cycle corresponds precisely with the extension of the Norwegian Trench. It is known that the annual cycle can show spatial complexity that depends on factors that include wind-driven barotropic processes in shallow semienclosed seas, and that coastal regions can be characterized by elevated amplitudes [*Vinogradov et al.*, 2008]. In this case, the evolution of the annual cycle amplitude with depth is in agreement with the circulation pattern of the region, characterized by a wide current in Danish Skagerrak and a narrow coastal current along the coast of Norway, whose extension in the open ocean is delimited by the presence of the deep Norwegian Trench. The high amplitudes of the annual cycle along the Norwegian coast of the Skagerrak Sea, captured also by the local TG, are less identifiable in the gridded product, probably due to its grid size.

5.4. Subbasin Estimation of the Annual Cycle

To get a more robust estimation of the annual cycle, the harmonic analysis has been performed by grouping the 1 Hz points of each track according to the corresponding subbasin. By doing so, the time series of each subbasin use multiple Envisat tracks and have a more frequent sampling, limiting the problem of the K1 aliasing period previously mentioned.

Figure 7 and Table 5 show the results of the annual cycle amplitude estimation performed with the PW estimator in each subbasin for the TGs, for Envisat altimetry at different distances from coast (from ALES reprocessed data set and SL_cci), and for the gridded SL_cci product.

The estimates from ALES altimetry points closest to the coast agree with the TG estimates to within 1 cm for all the subbasins with the exception of Norwegian Skagerrak, showing a significant improvement w.r.t. the comparison between TG and closest 1 Hz point estimates shown in Table 3. We can conclude that on a subbasin scale, the ALES reprocessed data set is able to give the most reliable coastal annual cycle amplitude estimations, and the improvements are particularly felt in the East and West Arkona subbasins. For the

Table 4. RMS Difference Between the Sinusoids Corresponding to the Annual Cycle of the Sea Level Estimated by the Tide Gauges and the Sinusoids Estimated From the Different Altimetry Data Sets for Each Subbasin[a]

Subbasin	ALES (m)	SL_cci Env (m)	SL_cci (m)	RADS (m)
Kattegat	0.012	0.019	0.006	0.023
Norway Skagerrak	0.014	0.022	0.023	0.028
Denmark Skagerrak	0.008	0.008	0.006	0.012
Sweden Skagerrak	0.008	0.010	0.007	0.013
West Arkona	0.004	0.031	−0.018	0.024
East Arkona	0.005	0.016	0.006	0.773
Belts	0.006	0.008	0.000	0.027

[a]Only data within 15 km of the coast.

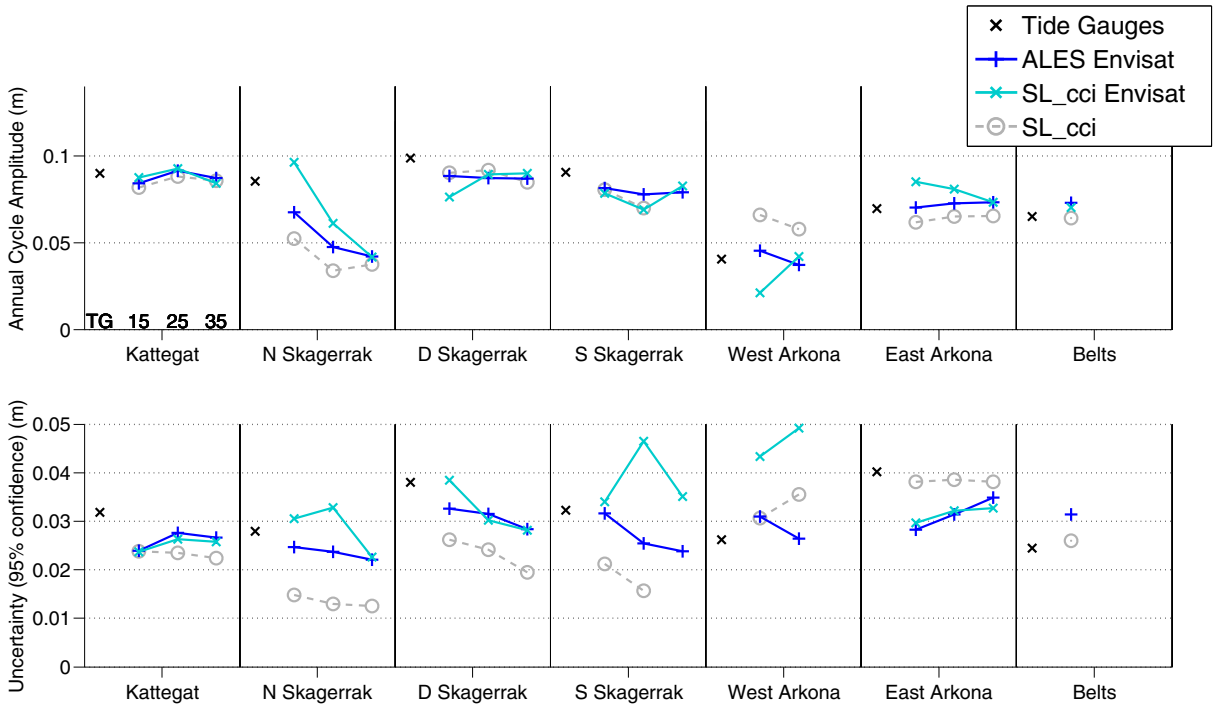

Figure 7. Estimates of the amplitude of the (top) annual cycle of the sea level and corresponding uncertainty at 95% level for each subbasin from TG data (black cross) and altimetry within 15 km of the coast, from 15 to 25 km and from 25 to 35 km (left to right in each subbasin box). The estimation is performed with the PW method. The estimates come from ALES reprocessed data set (blue), Envisat SL_cci (cyan), and gridded SL_cci (grey).

Norwegian Skagerrak, the increase of the annual amplitude from the deeper area to the coast is well represented by the transition from the ALES altimetry data to the TG.

The gradient of the amplitude of the annual cycle from the coast to the open sea is an important example of a characteristic that it is not possible to derive from a TG-based analysis. The gradient follows the

Table 5. Results of the PW Amplitude Estimation for the Annual Component of the Sea Level in the Years 2002–2010 for Each Subbasin[a]

Subbasin	Alt Data Set	Tide Gauges	Within15 km	15–25 km	25–35 km
Kattegat	ALES	0.090 ± 0.032	0.084 ± 0.024	0.091 ± 0.028	0.087 ± 0.027
	SL_cci Env	0.090 ± 0.032	0.087 ± 0.024	0.093 ± 0.026	0.084 ± 0.026
	SL_cci	0.090 ± 0.032	0.082 ± 0.024	0.088 ± 0.024	0.086 ±0.022
N Skagerrak	ALES	0.085 ± 0.028	0.067 ± 0.025	0.048 ± 0.024	0.041 ± 0.022
	SL_cci Env	0.085 ± 0.028	0.096 ± 0.030	0.061 ± 0.033	0.042 ± 0.023
	SL_cci	0.085 ± 0.028	0.052 ± 0.148	0.034 ± 0.013	0.037 ± 0.013
D Skagerrak	ALES	0.097 ± 0.038	0.088 ± 0.033	0.087 ± 0.032	0.087 ± 0.028
	SL_cci Env	0.097 ± 0.038	0.076 ± 0.039	0.089 ± 0.030	0.090 ± 0.028
	SL_cci	0.097 ± 0.038	0.090 ± 0.026	0.091 ± 0.024	0.085 ± 0.020
S Skagerrak	ALES	0.091 ± 0.032	0.081 ± 0.032	0.077 ± 0.026	0.080 ± 0.024
	SL_cci Env	0.091 ± 0.032	0.078 ± 0.034	0.069 ± 0.047	0.083 ± 0.035
	SL_cci	0.091 ± 0.032	0.081 ± 0.021	0.070 ± 0.016	–
West Arkona	ALES	0.040 ± 0.026	0.044 ± 0.031	0.037 ± 0.026	–
	SL_cci Env	0.040 ± 0.026	0.021 ± 0.043	0.042 ± 0.049	–
	SL_cci	0.040 ± 0.026	0.066 ± 0.031	0.058 ± 0.036	–
East Arkona	ALES	0.070 ± 0.040	0.070 ± 0.028	0.073 ± 0.032	0.073 ± 0.035
	SL_cci Env	0.070 ± 0.040	0.085 ± 0.030	0.081 ± 0.032	0.073 ± 0.033
	SL_cci	0.070 ± 0.040	0.062 ± 0.038	0.065 ± 0.039	0.065 ± 0.038
Belts	ALES	0.065 ± 0.024	0.073 ± 0.031	–	–
	SL_cci Env	0.065 ± 0.024	0.070 ± 0.050	–	–
	SL_cci	0.065 ± 0.024	0.064 ± 0.026	0.066 ± 0.021	–

[a]For each altimetry data set, i.e., ALES Envisat, SL_cci Envisat, and gridded SL_cci, the estimation is performed considering 1 Hz altimetry points within 15 km of the coast (coloumn 4), from 15 to 25 Km (column 5) and from 25 to 35 Km (column 6). The same PW estimation is applied to the tide gauges and reported in column 3. All the uncertainties are referred to the 95% confidence level.

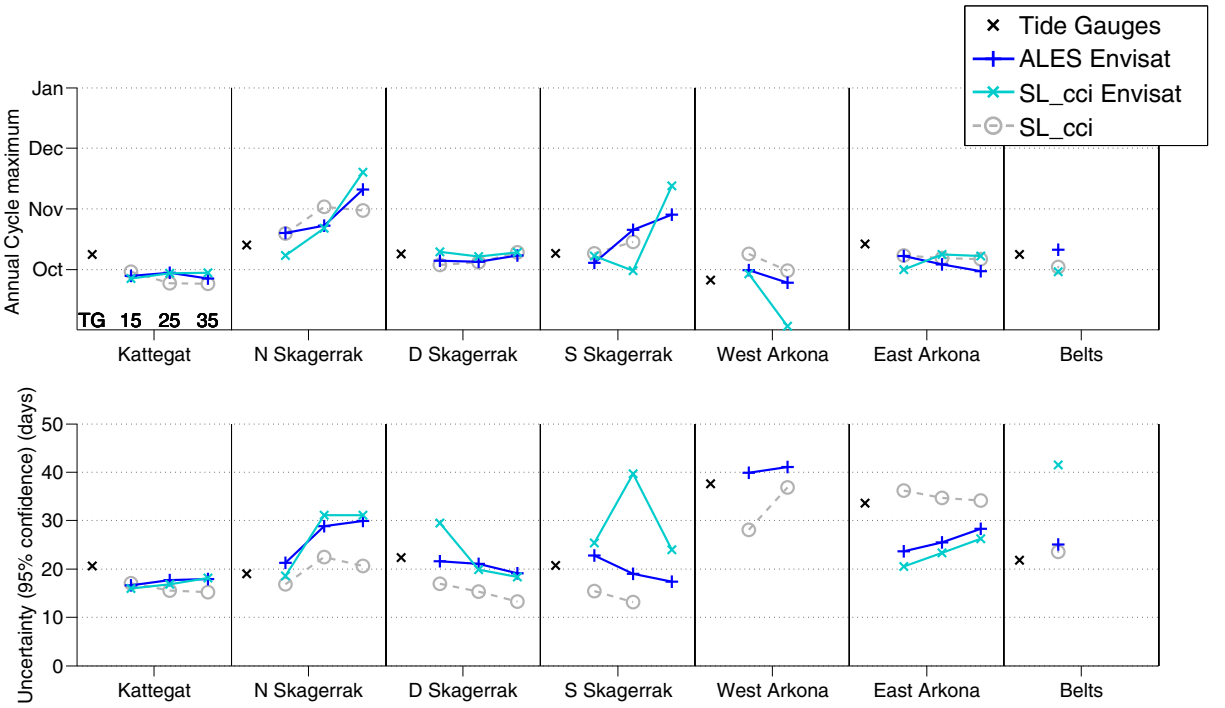

Figure 8. Estimates of the phase of the (top) annual cycle of the sea level and corresponding uncertainty at 95% level for each subbasin from TG data (black cross) and altimetry within 15 km of the coast, from 15 to 25 km and from 25 to 35 km (left to right in each subbasin box). The estimation is performed with the PW method. The estimates come from ALES reprocessed data set (blue), Envisat SL_cci (cyan), and gridded SL_cci (grey). The estimates correspond to timing of annual cycle maximum.

bathymetry of the area, which degrades from few meters to hundreds of meters of depth in few km (see Figure 1). The high coastal amplitude is very similar to the annual cycle of the Kattegat Sea and the shallow areas of the Skagerrak Sea. This is in accordance with the general circulation pattern, since the Norwegian Coastal Current is the returning flow of the Jutland current, which incorporates the outflow of the Kattegat Sea. The strong seasonal variability of the current has previously been noted in results from circulation models [*Maslowski and Walczowski*, 2002].

There is a clear border between the West and the East Arkona subbasins in terms of different amplitude of the annual cycle. In addition, it is known that the exchange of water between the Arkona and the Kattegat is different in the two subbasins, because they are well separated by the Darss Sill and, according to *Lass and Mohrholz* [2003], the exchange of water between the Kattegat and the Baltic Sea is faster and more direct through the Oresund Strait than through the channels in the Belts and the West Arkona subbasin. Further evidence of these differences is found in section 5.5 investigating temperature and salinity profiles.

Given the agreement of coastal data with tide gauge estimates, these results represent a step forward compared to previous analysis of the area, which avoided using coastal data due to the lack of validated products [*Madsen et al.*, 2007; *Stramska*, 2013; *Stramska et al.*, 2013].

In the bottom plot of Figure 7, the uncertainties are shown with the 95% confidence interval, which corresponds to roughly twice the standard error. They are generally smaller, but still of the same order of magnitude as the estimates, due to the short time series considered. The estimates from Envisat SL_cci data in the Belts and the West Arkona regions are exceptions, since uncertainties are higher due to the limited amount of valid data. Uncertainties of the estimates for TGs could be reduced by using high-frequency data rather than the monthly means provided by the PSMSL service. Concerning altimetry, the only feasible solution to increase the reliability is to extend the time series. The Jason series is currently the longest that it is possible to reprocess with the ALES retracker, but the coarser spatial coverage could affect the retrieval of differences between small subbasins, such as the West Arkona area considered in this study. The availability of missions that improve the density of tracks and with enhanced coastal capabilities, such as AltiKa, CryoSat-2 and soon Sentinel-3, is promising in terms of future extensions. The very recently completed reprocessing

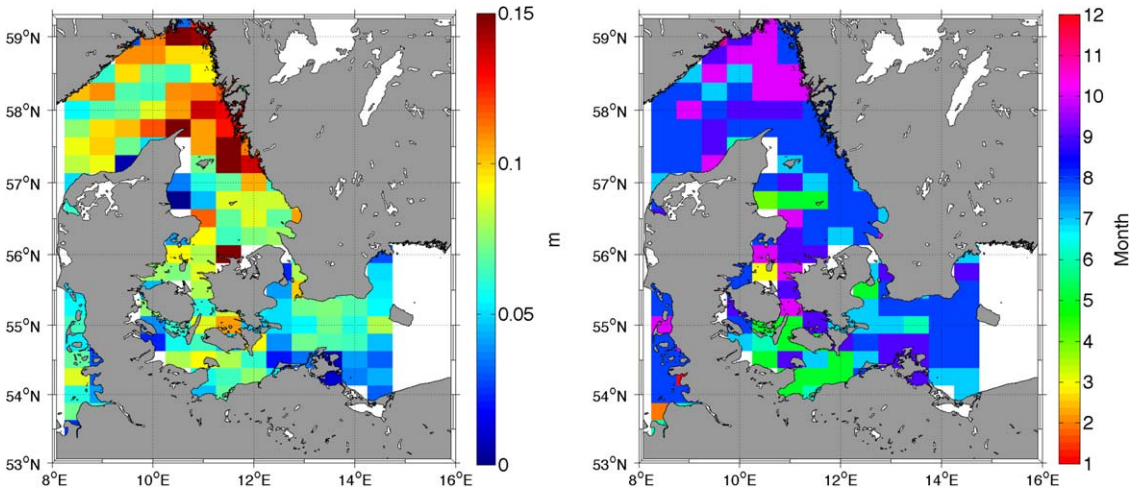

Figure 9. (left) Annual cycle amplitude and (right) month of the annual cycle maximum of the steric height derived from climatological data.

of the ERS-1/2 missions via the REAPER ("Reprocessing of Altimeter Products for ERS" [*Rudenko et al*., 2012]) study calls for a similar assessment of the coastal capabilities of such sensors.

The results of the phase estimation are shown in Figure 8. The points represent the period of the year when the maximum amplitude of the annual cycle occurs. Coastal estimates from ALES and SL_cci products are in agreement with TGs estimates within a few days in every subbasin. The maxima for all subbasins happen in late autumn. Considering only the wind stress driver, the sea level maxima would be expected later in winter, at the end of the season of strong westerlies that push water mass from the North Sea. On the other hand, the thermal expansion of the surface and subsurface waters in the Northern Hemisphere is expected at the end of the summer season. We argue that the late-autumn maxima are a consequence of the phase shift between the mass and the steric component of the annual cycle and we provide the verification in the next section.

Table 4 shows, for each subbasin, the RMS difference between the annual signal estimated by the averaged time series computed from the TGs and the annual signal estimated from the different altimetry data sets using the data within 15 km of the coast. As done previously, the TGs estimates represent the ground truth. In this way, it is possible to provide an objective evaluation that considers phase and amplitude at the same time. The sinusoids obtained from ALES coastal data are everywhere more similar to the signal derived from the TGs than the corresponding Envisat SL_cci estimations. Compared to the multimission gridded SL_cci, ALES improves the estimations in the Norway Skagerrak and in the West Arkona, while the gridded data set has a more accurate annual cycle estimation in the Belts and in the Kattegat. The sinusoids from ALES are the only data with an RMS difference that does not exceed 2 cm in every subbasin. The last column of the table shows the same statistics for RADS, whose RMS is higher than any of the other data sets in every subbasin, except for the West Arkona, where RADS scores slightly better than Envisat SL_cci. This proves that the improvements seen in the estimation of the annual cycle of the sea level from ALES are directly related to the quality of the retracked data and are not simply a consequence of different postprocessing techniques.

Ruiz Etcheverry et al. [2015] recently performed a similar study comparing the annual cycle from tide gauges and from AVISO gridded product in the same area (Figure 5 of the same article). In terms of RMS difference between the annual harmonics, they found agreement within $\sim$2 cm in the whole area, except in the West Arkona, where they found differences of over 4 cm. Our analysis in the same subbasin demonstrates not only that the SL_cci gridded product obtains better results, which might be due to the different corrections applied and/or to the different time frame considered, but also the significative improvement in RMS difference brought by the use of ALES data, which brings the statistics below the cm level.

Overall, the results obtained from the altimetry data set in this research stress the importance of dense data coverage in such high-variability areas. *Stramska* [2013] referred the annual cycle of the Baltic Sea detected

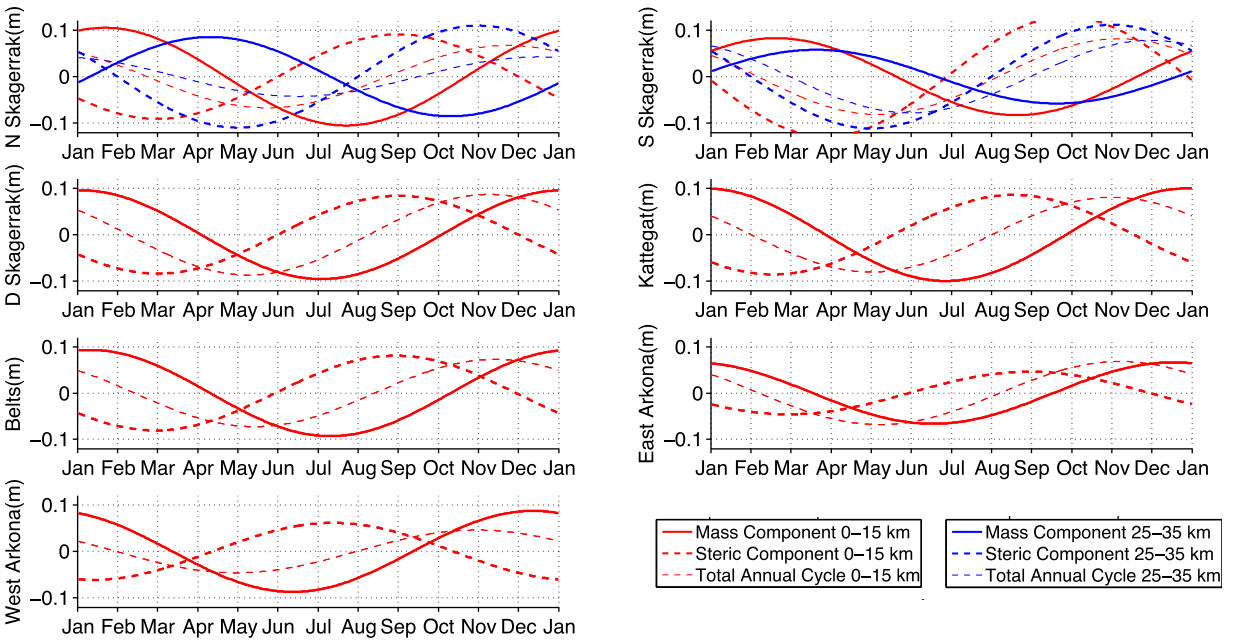

Figure 10. Estimates of the sinusoidal signal related to the annual cycle of the mass component of the sea level variability (thick line) for each subbasin, obtained by subtracting the steric annual signal (estimated from climatology, thick dashed line) from the total annual signal (estimated from ALES data set, thin dashed line). Estimates are computed from data within 15 km of the coast (red) and from 25 to 35 km (blue).

by satellite altimetry to a single point in the open sea; our research argues that a subbasin analysis from the coast to the open sea is reliable (as confirmed by the comparison with the tide gauges) and it highlights considerable differences in the amplitude of the annual cycle within different areas of the Baltic Sea (West Arkona, East Arkona).

5.5. Climatology and Steric Component of the Annual Cycle

We have also derived the annual cycle of the steric height from in situ observations stored in a climatologic data set [*Bersch et al.*, 2013] in order to further improve understanding of the mechanisms driving the annual cycle in sea level and to provide explanations to points raised in the previous section.

Figure 9 shows the annual cycle amplitude (left) and the month of the maximum in the steric height annual cycle (right) derived from climatological data.

The amplitude of the annual cycle for the steric component is higher in the Skagerrak Sea than in the rest of the domain and reaches the highest values in the transition zone between the Skagerrak Sea and the Kattegat Sea, where there are the strongest variations of the water column characteristics depending on the penetration of different waters (warmer and more saline from the Atlantic or colder and brackish from the Baltic) into the area.

Despite the coarse grid, it is evident that the dynamics in the coastal zone of the Skagerrak Sea are different than in the Norwegian Trench, as already seen in the total sea level annual cycle: the areas with the strongest seasonality follow the circulation pattern of the Jutland Current and the NCC. Nevertheless it has to be noted that some strong shifts in amplitude and phase within adjacent gridpoints are unrealistic and may be a consequence of the unequal sampling of the data set, both in time and space.

The steric height is maximum in August/September in most of the area, as a consequence of the warming of the first layers of water. The Arkona basin has a distinct phase shift in the steric height annual cycle from the west to the east. The average thermosteric annual cycle (not shown) in the whole Arkona basin has a maximum in August and an amplitude of about 3.5 cm. But the average halosteric component in the West Arkona has an amplitude of 6 cm and a maximum in May, compared to an amplitude of 3 cm and a maximum in late June in East Arkona. The halosteric component of the West Arkona is strongly influenced by the haline Kattegat water influx events, which are more common in autumn/winter [*Lehmann*, 1995]. In West Arkona therefore, due to the strong halosteric component, the phase of the steric component is

almost in opposition to the phase of the mass component: as a consequence, the amplitude of the total annual cycle in West Arkona is significantly smaller than in the other subbasins, as seen in Figures 6 and 7.

The information coming from the climatology gives us key information to interpret the annual cycle derived from satellite altimetry. It is evident that there is a strong mass component that influences the total annual cycle of the sea level, given that the steric cycle is not able to explain entirely the annual signal from altimetry, neither in phase nor in amplitude. By subtracting the steric annual signal from the total annual signal, we have attempted to estimate the mass component. Figure 10 shows the three sinusoids for each subbasin. The total annual signal was obtained using the ALES coastal time series within 15 km of the coast and the steric component comes from the climatological data just described. As expected, in all the subbasins, the mass component has a winter maximum, coincident with the season of strongest winds, with an amplitude ranging from $\sim$7 to $\sim$10 cm. The estimations farther from the coast are not shown because they have very similar values; an exception is made for Norwegian and Swedish Skagerrak, where the deeper areas of the Norwegian Trench have a later maximum. This could be due to the presence of an intermediate water layer between about 50 and 300 m, which is warmer in late autumn and early winter than in summer: this phenomenon has been described in *Danielssen et al*. [1996] and is caused by the penetration of warmer mass from the Atlantic in the Skagerrak Sea and its longer residence time in the intermediate layer. The overall delayed steric height phase in a deep area such as the Norwegian Trench has a direct consequence on the total sea level phase from satellite altimetry, as shown in Figure 8. The use of gravimetery-derived mass measurements by means of data from GRACE mission, which has recently been attempted in basins of similar scales (the Red Sea, in *Wahr et al*. [2014]) could quantitatively assess the mass contribution to the annual cycle and help in validating our attempt.

6. Conclusions

We have tested the suitability of satellite altimetry from the Envisat mission to perform regional analysis of sea level in shallow seas and coastal areas. The analysis was focused on the annual signal of the intersection between the North Sea and the Baltic Sea. Data from a dedicated coastal altimetry processing (ALES) were compared with data from the SL_cci project and the RADS archive, and verified in the coastal zone using data from TGs.

We have shown that ALES retracking and improved corrections increase the amount and the quality of sea level retrievals in the area of study, allowing a more accurate estimation of the annual cycle up to the coast. Only ALES-based amplitude estimates of the annual cycle are in agreement with TGs within 1 cm in every subbasin with the exception of the Norwegian coast of the Skagerrak Sea. Here the difference between ALES and TG estimates of the annual cycle allows the recognition of a slope in the amplitude that follows the bathymetry of the Skagerrak sea and is not well represented in the SL_cci estimates. The estimates of the annual cycle of the sea level from Level 4 gridded SL_cci product are in agreement with the TGs in most locations, but overestimate the amplitude in the West Arkona basin, probably due to residual tidal variability, and lack coastal details in the Norwegian Skagerrak, probably due to the gridding and the exclusion of coastal sea level retrievals.

We have also identified the sources of the variability in the annual cycle of the sea level considering external information. The sea level time series in the period 2002–2010 are correlated with the large-scale wind pattern. The advection of water masses into/out of the Skagerrak and the Kattegat Sea due to westerly/easterly winds is shown to be the dominant regulator of the coastal annual cycle and the interannual sea level variations. The differences within and among the subbasins are driven by different phases of the steric cycle (West Arkona and Norwegian Trench) and by coastal circulation patterns (Norwegian Coastal Current).

This study demonstrates that coastal altimetry is now in a mature stage in which it can be used for coastal sea level variability studies at subregional spatial scales and annual time scales. Sea level studies should use reprocessed coastal altimetry with confidence also in areas where in situ data are absent. The methodology applied in this paper is potentially applicable to other coastal areas, providing that the aliased annual component of tidal constituents such as K1 for Envisat is of a lower order of magnitude of the annual cycle of the sea level. The subbasin division can increase the frequency of the measurements in a time series and limit aliasing problems in the annual cycle estimates due to the Envisat repeat orbit. Nevertheless, this

procedure requires an a priori knowledge of the dynamics of the area and an along-track analysis can help to detect differences within each subbasin, particularly in areas with bathymetry slopes.

In this research, ALES algorithm has improved the sea level estimates in the coastal regions w.r.t. comparable along-track data sets. Future research should address the reprocessing of previous missions (ERS, Topex) in order to extend the coastal sea level time series, as well as the coastal performances of the new generation of altimeters (CryoSat-2, Sentinel 3, Sentinel 6) with and without a dedicated coastal retracker.

Acknowledgments

Sensor Geophysical Data Records (SGDR) of Envisat were obtained from Earth Online (EO) User Services. The ESA SL CCI data were obtained by online request through the portal http://www.esa-sealevel-cci.org/ (version 1.1, released in December 2014). The Dynamic Atmosphere Correction has been downloaded from http://www.aviso.altimetry.fr. The GPD Wet Tropospheric Correction was provided courtesy of M. J. Fernandes (University of Porto, Portugal). DTU10 tide model and DTU13 mean sea surface have been downloaded from http://www.space.dtu.dk/. Tide gauges data are available at http://www.psmsl.org. Wind stress has been extracted from the SODA reanalysis product, version 2.2.4, downloaded from http://dsrs.atmos.umd.edu/. The KLIWAS climatology was downloaded from http://icdc.zmaw.de/. The authors would like to thank Ivan D. Haigh, Helen M. Snaith, Graham D. Quartly, and Kristine Madsen for their suggestions and genuine interest.

References

Alvera-Azcárate, A., D. Sirjacobs, A. Barth, and J.-M. Beckers (2012), Outlier detection in satellite data using spatial coherence, *Remote Sens. Environ.*, *119*, 84–91.

Andersen, O. (2010), The DTU10 gravity field and mean sea surface, paper presented at Second International Symposium of the Gravity Field of the Earth (IGFS2), Univ. of Alaska Fairbanks, Fairbanks.

Andersen, O. B., and R. Scharroo (2011), Range and geophysical corrections in coastal regions and implications for mean sea surface determination, in *Coastal Altimetry*, edited by S. Vignudelli et al., pp. 103–145, Springer, Berlin.

Andersen, O. B., A. Abulaitijiang, and L. Stenseng (2014), MSS at the coast. What Cryosat-2 revealed about existing MSS + Ocean Tide models in coastal & Arctic regions, paper presented at the 8th Coastal Altimetry Workshop, Konstanz, Germany.

Barbosa, S., M. Silva, and M. Fernandes (2008), Changing seasonality in North Atlantic coastal sea level from the analysis of long tide gauge records, *Tellus, Ser. A*, *60*(1), 165–177.

Bersch, M., V. Gouretski, R. Sadikni, and I. Hinrichs (2013), KLIWAS North Sea climatology of hydrographic data (version 1.0), World Data Cent. for Clim., doi:10.1594/WDCC/KNSC_hyd_v1.0.

Bonnefond, P., B. Haines, and C. Watson (2011), In situ absolute calibration and validation: A link from coastal to open-ocean altimetry, in *Coastal Altimetry*, edited by S. Vignudelli et al., pp. 259–296, Springer, Berlin.

Carrère, L., and F. Lyard (2003), Modeling the barotropic response of the global ocean to atmospheric wind and pressure forcing-comparisons with observations, *Geophys. Res. Lett.*, *30*(6), 1275, doi:10.1029/2002GL016473.

Cheng, Y., and O. B. Andersen (2011), Multimission empirical ocean tide modeling for shallow waters and polar seas, *J. Geophys. Res.*, *116*, C11001, doi:10.1029/2011JC007172.

Cipollini, P. (2011), A new parameter to facilitate screening of coastal altimetry data and corrections, paper presented at the 5th Coastal Altimetry Workshop, San Diego, Calif.

Danielssen, D. S., E. Svendsen, and M. Ostrowski (1996), Long-term hydrographic variation in the Skagerrak based on the section Torungen–Hirtshals, *ICES J. Mar. Sci.*, *53*(6), 917–925.

Ekman, M. (2009), *The Changing Level of the Baltic Sea During 300 Years: A Clue to Understanding the Earth*, Summer Inst. for Hist. Geophys., Åland Islands.

Envisat-1 Products Specifications (2009), *MWR Products Specifications: PO-RS-MDA-GS-2009. Rev. C.*, vol. 13.

Faugere, Y., J. Dorandeu, F. Lefevre, N. Picot, and P. Femenias (2006), Envisat ocean altimetry performance assessment and cross-calibration, *Sensors*, *6*(3), 100–130.

Giese, B. S., and S. Ray (2011), El Niño variability in simple ocean data assimilation (SODA), 1871–2008, *J. Geophys. Res.*, *116*, C02024, doi:10.1029/2010JC006695.

Gill, A. E. (1982), *Atmosphere-Ocean Dynamics*, vol. 30, Academic, San Diego, Calif.

Holt, J., and R. Proctor (2008), The seasonal circulation and volume transport on the northwest European continental shelf: A fine-resolution model study, *J. Geophys. Res.*, *113*, C06021, doi:10.1029/2006JC004034.

Ivchenko, V., S. Danilov, D. Sidorenko, J. Schröter, M. Wenzel, and D. Aleynik (2007), Comparing the steric height in the Northern Atlantic with satellite altimetry, *Ocean Sci. Discuss.*, *4*(3), 441–457.

Jayne, S. R., J. M. Wahr, and F. O. Bryan (2003), Observing ocean heat content using satellite gravity and altimetry, *J. Geophys. Res.*, *108*(C2), 3031, doi:10.1029/2002JC001619.

Joana Fernandes, M., C. Lazaro, A. L. Nunes, N. Pires, L. Bastos, and V. B. Mendes (2010), GNSS-Derived path delay: An approach to compute the Wet Tropospheric Correction for coastal altimetry, *IEEE Geosci. Remote Sens. Lett.*, *7*(3), 596–600, doi:10.1109/LGRS.2010.2042425.

Joana Fernandes, M., N. Pires, C. Lázaro, and A. Nunes (2013), Tropospheric delays from GNSS for application in coastal altimetry, *Adv. Space Res.*, *51*(8), 1352–1368.

Karagali, I., A. Peña, M. Badger, and C. B. Hasager (2014), Wind characteristics in the North and Baltic seas from the QuikSCAT satellite, *Wind Energy*, *17*(1), 123–140.

Lass, H., and V. Mohrholz (2003), On dynamics and mixing of inflowing saltwater in the Arkona Sea, *J. Geophys. Res.*, *108*(C2), 3042, doi:10.1029/2002JC001465.

Legeais, J.-F., M. Ablain, and S. Thao (2014), Evaluation of wet troposphere path delays from atmospheric reanalyses and radiometers and their impact on the altimeter sea level, *Ocean Sci.*, *10*(6), 893–905.

Lehmann, A. (1995), A three-dimensional baroclinic eddy-resolving model of the Baltic Sea, *Tellus, Ser. A*, *47*(5), 1013–1031.

Lehmann, A., W. Krauß, and H.-H. Hinrichsen (2002), Effects of remote and local atmospheric forcing on circulation and upwelling in the Baltic Sea, *Tellus, Ser. A*, *54*(3), 299–316.

Liebsch, G., K. Novotny, R. Dietrich, and C. Shum (2002), Comparison of multimission altimetric sea-surface heights with tide gauge observations in the Southern Baltic Sea, *Mar. Geod.*, *25*(3), 213–234.

Lombard, A., A. Cazenave, P.-Y. Le Traon, and M. Ishii (2005), Contribution of thermal expansion to present-day sea-level change revisited, *Global Planet. Change*, *47*(1), 1–16.

Madsen, K., J. Høyer, and C. Tscherning (2007), Near-coastal satellite altimetry: Sea surface height variability in the North Sea–Baltic Sea area, *Geophys. Res. Lett.*, *34*, L14601, doi:10.1029/2007GL029965.

Maslowski, W., and W. Walczowski (2002), Circulation of the Baltic Sea and its connection to the Pan-Arctic region-a large scale and high-resolution modeling approach, *Boreal Environ. Res.*, *7*(4), 319–326.

Novotny, K., G. Liebsch, A. Lehmann, and R. Dietrich (2006), Variability of sea surface heights in the Baltic sea: An intercomparison of observations and model simulations, *Mar. Geod.*, *29*(2), 113–134.

Passaro, M., P. Cipollini, S. Vignudelli, G. Quartly, and H. Snaith (2014), ALES: A multi-mission subwaveform retracker for coastal and open ocean altimetry, *Remote Sens. Environ.*, *145*, 173–189, doi:10.1016/j.rse.2014.02.008.

Passaro, M., L. Fenoglio-Marc, and P. Cipollini (2015), Validation of significant wave height from improved satellite altimetry in the German Bight, *IEEE Trans. Geosci. Remote Sens.*, *53*(4), 2146–2156, doi:10.1109/TGRS.2014.2356331.

Prais, S. J., and C. B. Winsten (1954), Trend estimators and serial correlation, Cowles Commission discussion paper no. 383, technical report, Chicago.

Rudenko, S., M. Otten, P. Visser, R. Scharroo, T. Schöne, and S. Esselborn (2012), New improved orbit solutions for the ers-1 and ers-2 satellites, *Adv. Space Res.*, *49*(8), 1229–1244.

Ruiz Etcheverry, L., M. Saraceno, A. Piola, G. Valladeau, and O. Möller (2015), A comparison of the annual cycle of sea level in coastal areas from gridded satellite altimetry and tide gauges, *Cont. Shelf Res.*, *92*, 87–97.

Samuelsson, M., and A. Stigebrandt (1996), Main characteristics of the long-term sea level variability in the Baltic sea, *Tellus, Ser. A*, *48*(5), 672–683.

Scharroo, R., E. W. Leuliette, J. L. Lillibridge, D. Byrne, M. C. Naeije, and G. T. Mitchum (2012), RADS: Consistent multi-mission products, paper SP-710 presented at the Symposium on 20 Years of Progress in Radar Altimetry, ESA, Venice, Italy, 20–28 Sept.

Stammer, D., et al. (2013), Accuracy assessment of global ocean tide models, paper presented at the Ocean Surface Topography Science Team Meeting, Boulder, Colo.

Stigebrandt, A. (1984), Analysis of an 89-year-long sea level record from the Kattegat with special reference to the barotropically driven water exchange between the Baltic and the sea, *Tellus, Ser. A*, *36*(4), 401–408.

Stramska, M. (2013), Temporal variability of the Baltic Sea level based on satellite observations, *Estuarine Coastal Shelf Sci.*, *133*, 244–250.

Stramska, M., and N. Chudziak (2013), Recent multiyear trends in the Baltic Sea level, *Oceanologia*, *55*(2), 319–337.

Stramska, M., H. Kowalewska-Kalkowska, and M. Swirgon (2013), Seasonal variability in the Baltic Sea level, *Oceanologia*, *55*(4), 787–807.

Svendsen, E., J. Bemtsen, M. Skogen, B. Ådlandsvik, and E. Martinsen (1996), Model simulation of the Skagerrak circulation and hydrography during SKAGEX, *J. Mar. Syst.*, *8*(3), 219–236.

Tomczak, M., and J. S. Godfrey (2003), *Regional Oceanography: An Introduction*, Daya Publishing House, Delhi, India.

Vignudelli, S., A. G. Kostianoy, P. Cipollini, and J. Benveniste (2011), *Coastal Altimetry*, Springer-Verlag, Berlin Heidelberg.

Vinogradov, S., and R. Ponte (2010), Annual cycle in coastal sea level from tide gauges and altimetry, *J. Geophys. Res.*, *115*, C04021, doi: 10.1029/2009JC005767.

Vinogradov, S. V., R. M. Ponte, P. Heimbach, and C. Wunsch (2008), The mean seasonal cycle in sea level estimated from a data-constrained general circulation model, *J. Geophys. Res.*, *113*, C03032, doi:10.1029/2007JC004496.

Volkov, D. L., M. Pujol, et al. (2012), Quality assessment of a satellite altimetry data product in the Nordic, Barents, and Kara seas, *J. Geophys. Res.*, *117*, C03025, doi:10.1029/2011JC007557.

Wahl, T., I. Haigh, P. Woodworth, F. Albrecht, D. Dillingh, J. Jensen, R. Nicholls, R. Weisse, and G. Wöppelmann (2013), Observed mean sea level changes around the North Sea coastline from 1800 to present, *Earth Sci. Rev.*, *124*, 51–67.

Wahr, J., D. A. Smeed, E. Leuliette, and S. Swenson (2014), Seasonal variability of the Red Sea, from satellite gravity, radar altimetry, and in situ observations, *J. Geophys. Res. Oceans.*, *119*, 5091–5104, doi:10.1002/2014JC010161.

Winther, N. G., and J. A. Johannessen (2006), North Sea circulation: Atlantic inflow and its destination, *J. Geophys. Res.*, *111*, C12018, doi: 10.1029/2005JC003310.